On the Effect of the Atmosphere on the Evaporation of Sessile Droplets of Water

K. Sefiane[1], S. K. Wilson[2*], S. David[1], G. J. Dunn[2], and B. R. Duffy[2]

[1]*School of Engineering, The University of Edinburgh,*

The King's Buildings, Mayfield Road,

Edinburgh EH9 3JL, United Kingdom

[2]*Department of Mathematics, University of Strathclyde,*

Livingstone Tower, 26 Richmond Street,

Glasgow G1 1XH, United Kingdom

(Dated: 6th November 2008, revised 3rd March and 3rd April 2009)

Abstract

An experimental and theoretical study into the effect of the atmosphere on the evaporation of pinned sessile droplets of water is described. The experimental work investigated the evaporation rates of sessile droplets in atmospheres of three different ambient gases (namely, helium, nitrogen and carbon dioxide) at reduced pressure (from 40 to 1000 mbar) using four different substrates (namely, aluminium, titanium, Macor and PTFE) with a wide range of thermal conductivities. Reducing the atmospheric pressure increases the diffusion coefficient of water vapour in the atmosphere and hence increases the evaporation rate. Changing the ambient gas also alters the diffusion coefficient and hence also affects the evaporation rate. A mathematical model that takes into account the effect of the atmospheric pressure and the nature of the ambient gas on the diffusion of water vapour in the atmosphere and the thermal conductivity of the substrate is developed, and its predictions are found to be in encouraging agreement with the experimental results.

* Author for correspondence. Email: s.k.wilson@strath.ac.uk, Telephone: + 44 (0) 141 548 3820, Fax: + 44 (0) 141 548 3345.

I. INTRODUCTION

When liquid droplets are deposited on a solid substrate in an unsaturated atmosphere they will experience some degree of evaporation. This apparently simple phenomenon is encountered in everyday life as well as in a wide range of physical and biological processes, and was studied more than a century ago by Maxwell[1] and Langmuir[2]. However, over the last decade renewed interest in the subject has been sparked by new developments in applications such as cooling technologies, desalination, painting, DNA synthesis and patterning technologies. Unlike in the case of aerosol droplets, in the case of sessile droplets three phases co-exist: solid (substrate), liquid (droplet) and gas (atmosphere). A full understanding of the physics and controlling mechanisms for evaporating sessile droplets thus requires a thorough analysis of the heat and mass transfer across the interfaces as well as the interaction between the three phases.

Extensive studies of the evaporation of sessile droplets have been undertaken to elucidate the underlying mechanisms, notably those by Picknett and Bexon[3] and Bourges-Monnier and Shanahan[4]. While there are situations in which the contact line of the droplet moves throughout the evaporation process (for example, Poulard et al.[5] studied the evaporation of droplets of completely wetting liquids with receding contact lines), typically it is found that on real (i.e. rough) surfaces the contact line remains pinned for much of the lifetime of the droplet. Deegan[6] investigated the evaporation of pinned droplets and the formation of the so-called "ring stain" or "coffee stain" that can occur. The standard theoretical model used by Picknett and Bexon[3], Deegan[6], Hu and Larson[7] and Popov[8] and several others (hereafter referred to as the "basic model") assumes that the rate-limiting mechanism for evaporation is the diffusive relaxation of the locally saturated vapour at the free surface of the droplet to its far-field value (which occurs on a timescale of 10^{-4} s over 100 μm for water vapour in air; see, for example, Poulard et al.[9]) and not the much faster transfer rate of molecules across the interface itself (which occurs on a timescale of 10^{-10} s; see, for example, Popov[8]). Recently Shahidzadeh-Bonn et al.[10] studied evaporating droplets of organic liquids and of water, and suggested that, unlike for organic liquids, evaporation of water may not be simply diffusive. Specifically, they suggested that, because water vapour is less dense than air (whereas the vapour of organic liquids is more dense than air) buoyancy effects may be significant in the evaporation of droplets of water. However, more recently, Guéna et

al.[11] compared the evaporation of small pendant (i.e. hanging) and sessile droplets of water and found the results to be identical, raising questions about the role of buoyancy. The basic model predicts that the evaporation is integrably singular at the contact line and that the overall evaporation rate is proportional to the perimeter of the base of the droplet, in agreement with experimental studies such as that by Birdi et al.[12]. However, the basic model decouples the concentration of vapour in the atmosphere from the temperature of the droplet and the substrate, and hence does not account for the effect of the thermal properties of the droplet and the substrate on the evaporation rate. Indeed, it is fair to say that until recently the role of the thermal properties of the substrate has been more or less overlooked: different investigators have conducted experiments on different substrates to reach general conclusions without fully taking into account the influence of the thermal properties of the substrate. However, recently David et al.[13] carried out an experimental investigation of evaporating droplets of various liquids on a variety of substrates with different thermal properties. David et al.[13] showed that the evaporation rate of such droplets varies significantly with the thermal conductivity of the substrate. Dunn et al.[14,15] developed a mathematical model for the evaporation of a droplet on a substrate taking into account the temperature dependence of the saturation concentration of vapour at the free surface of the droplet, and found that its predictions are in excellent quantitative agreement with the experimental results of David et al.[13].

The theory describing diffusion in binary gas mixtures is well developed. Solving the Boltzmann equation, Reid et al.[16] derived the following theoretical expression for the diffusion coefficient in a binary gas system:

$$D_{\mathrm{AB}} = \frac{3}{16}\frac{(4\pi KT/M_{\mathrm{AB}})^{1/2}}{n\pi\sigma_{\mathrm{AB}}^2\Omega_{\mathrm{D}}}f_{\mathrm{D}}, \tag{1}$$

which, with the ideal gas law, may be rewritten as

$$D_{\mathrm{AB}} = \frac{0.00266T^{3/2}}{PM_{\mathrm{AB}}^{1/2}\sigma_{\mathrm{AB}}^2\Omega_{\mathrm{D}}}f_{\mathrm{D}}, \tag{2}$$

where D_{AB} denotes the diffusion coefficient of gas A into gas B, M_{A} and M_{B} the molecular weights of gas A and gas B, $M_{\mathrm{AB}} = 2[1/M_{\mathrm{A}} + 1/M_{\mathrm{B}}]^{-1}$, n is the number density of molecules in the mixture, K is Boltzmann's constant, T is the absolute temperature, σ_{AB} is the characteristic length related to the size of the diffusing molecules, Ω_{D} is the diffusion collision integral, f_{D} is a correction term, and P is the pressure. In particular, equation (2) reveals that the diffusion coefficient is proportional to $T^{3/2}$ and inversely proportional to P.

Another important effect related to the phase-change process is evaporative cooling. Ward and Duan[17] investigated the cooling induced during the evaporation of water in an atmosphere of water vapour at reduced pressure. Substantial cooling of the liquid interface was reported and the temperature drop was found to increase with increasing evaporation rates.

The objective of the present work is to investigate the effect of the atmosphere on the evaporation of pinned sessile droplets of water. The results are presented for droplets in atmospheres of three different ambient gases (namely, helium, nitrogen and carbon dioxide) at reduced pressure using four different substrates (namely, aluminium, titanium, Macor and PTFE) with a wide range of thermal conductivities. A mathematical model that takes into account the effect of the atmosphere and the substrate is developed, and its predictions are found to be in encouraging agreement with the experimental results.

II. EXPERIMENTAL SET UP AND PROCEDURE

The essence of the experiment consisted of depositing a liquid droplet of controlled volume on a substrate and allowing it to evaporate spontaneously. All of the experiments reported here were realised with droplets of pure deionised water resting on four different substrates chosen for their wide range of thermal conductivities, namely aluminium (Al), titanium (Ti), Macor and PTFE. The substrates had dimensions of 10 mm $\times$ 10 mm $\times$ 1 mm (length $\times$ width $\times$ thickness), and the thermal conductivities of the substrates used in the experiments are given in Table I.

Two instruments were used to characterise the surface properties of substrates. These two instruments are complementary as they characterise the surface at two different scales: a NewView 100$^{\mathrm{TM}}$ from ZYGO Corporation which uses scanning white light interferometry (SWLI), and an MFP-1D$^{\mathrm{TM}}$ Atomic Force Microscope (AFM) from Asylum Research which uses contact force microscopy (CFM). All of the substrates were found to be relatively rough, and the contact lines of the droplets were found to be pinned during the first stage of the evaporation process.

In order to contain the ambient gas and to vary the atmospheric pressure, the experiments were performed in a "low pressure" chamber, shown in Figure 1. The chamber was a cell which is cylindrical in shape (105 mm diameter and 95 mm height) connected to a gas supply and a vacuum pump. Two observation windows (each 40 mm in diameter), located

Substrate	Al	Ti	Macor	PTFE
Thermal Conductivity (W m^{-1} K^{-1})	237	21.9	1.46	0.25

TABLE I: The thermal conductivities of the substrates used in the experiments, k^s, taken from David et al.[13].

Ambient Gas	He	N_2	CO_2
Diffusion Coefficient (m^2 s^{-1})	8.26×10^{-5}	2.47×10^{-5}	1.45×10^{-5}

TABLE II: The reference values of the diffusion coefficients of water vapour into the ambient gases used in the experiment, D_{ref}, at pressure 1 atm and temperature 295 K, obtained from Reid et al.[16].

on opposite sides of the chamber, allowed lighting and visual inspection as well as video recording. The experimental setup used a DSA100$^{\text{TM}}$ Droplet Shape Analysis (DSA) system from KRÜSS GmbH on which the low pressure chamber was mounted, and is shown in Figure 2. The DSA100$^{\text{TM}}$ system, consisting of both hardware (including a light source, an injection system, a charge-coupled device (CCD) camera, and a three-axis stage) and DSA software (including both injection controller and image analysis software), was used to measure the droplet profile optically. Specifically, the DSA100$^{\text{TM}}$ system was used to measure the base radius, maximum height, contact angle and volume of the droplet as functions of time, and then the evaporation rate was calculated from the rate of change of the volume of the droplet. The accuracy of this procedure was confirmed by David et al.[13] and Dunn et al.[15], both of whom also made direct measurements of the droplet volume using an analytical balance. Typical examples of the droplet and of the experimentally measured evolutions of the volume and the base radius are shown in Figures 3 and 4, respectively. All of the experiments were carried out in a laboratory in which the room temperature was controlled at 295 K with an air-conditioning unit with a precision of ± 1 K. Before each experiment, air was removed from the chamber and replaced with the chosen ambient gas. The pressure of the gas was varied in the range 40 to 1000 mbar. Since the diffusion coefficient of water vapour in the atmosphere depends on the nature of the ambient gas as well as on its pressure, it was decided also to vary the ambient gas. The experiments were therefore carried out using three different ambient gases, namely helium (He), nitrogen (N_2) and carbon dioxide (CO_2), chosen for their different diffusion coefficients. The reference values of the diffusion

coefficients of the ambient gases used in the experiments are given in Table II.

In order to quantify the amount of evaporative cooling of a droplet relative to the atmospheric temperature, the bulk temperature inside the droplet was measured with a miniature thermocouple which was inserted into the droplet near its apex along the vertical axis, as shown in Figure 5. The thermocouple was 100 μm in size, and, as Figure 5 shows, the perturbation to the droplet due to the thermocouple was minimal.

III. MATHEMATICAL MODEL

The mathematical model used in the present work represents the quasi-steady diffusion-limited evaporation of a pinned axisymmetric droplet of Newtonian fluid with constant viscosity, density ρ, surface tension γ, and thermal conductivity k resting on a horizontal substrate of constant thickness h^{s} with constant thermal conductivity k^{s}. Referred to cylindrical polar coordinates (r, θ, z) with origin on the substrate at the centre of the droplet with the z axis vertically upwards, the shape of the free surface of the droplet at time t is denoted by $z = h(r, t)$, the upper surface of the substrate by $z = 0$, and the lower surface of the substrate by $z = -h^{\mathrm{s}}$, as shown in Figure 6.

For a sufficiently small droplet[18], the droplet shape can be approximated as a simple quasi-steady spherical cap,

$$h = \sqrt{\frac{R^2}{\sin^2\theta} - r^2} - \frac{R}{\tan\theta}, \tag{3}$$

and hence the relation between the volume $V = V(t)$ and the contact angle $\theta = \theta(t)$ is given by

$$V = \frac{\pi h_{\mathrm{m}}(3R^2 + h_{\mathrm{m}}^2)}{6}, \tag{4}$$

where R and $h_{\mathrm{m}} = h_{\mathrm{m}}(t) = h(0, t) = R\tan(\theta/2)$ are the base radius and the maximum height of the droplet, respectively. The total evaporation rate is given by

$$-\frac{\mathrm{d}V}{\mathrm{d}t} = \frac{2\pi}{\rho}\int_0^R J\sqrt{1 + \left(\frac{\partial h}{\partial r}\right)^2}\, r\,\mathrm{d}r, \tag{5}$$

where $J = J(r, t)\,(\geq 0)$ is the local evaporative mass flux from the droplet.

The atmosphere in the chamber surrounding the droplet and the substrate is assumed to be at constant atmospheric temperature T_{a} and atmospheric pressure p_{a}. The temperatures of the droplet and the substrate, denoted by $T = T(r, z, t)$ and $T^{\mathrm{s}} = T^{\mathrm{s}}(r, z, t)$, respectively,

satisfy Laplace's equation $\nabla^2 T = \nabla^2 T^{\rm s} = 0$. The mass flux from the droplet satisfies the local energy balance

$$\mathcal{L} J = -k \nabla T \cdot \mathbf{n} \quad \text{on} \quad z = h \quad \text{for} \quad r < R, \tag{6}$$

where $\mathcal{L}$ is the latent heat of vaporisation and $\mathbf{n}$ is the unit outward normal to the free surface of the droplet. We assume that the temperature and the heat flux are continuous between the droplet and the substrate,

$$T = T^{\rm s} \quad \text{and} \quad -k \frac{\partial T}{\partial z} = -k^{\rm s} \frac{\partial T^{\rm s}}{\partial z} \quad \text{on} \quad z = 0 \quad \text{for} \quad r < R, \tag{7}$$

and that the temperature is continuous between the substrate and the atmosphere,

$$T^{\rm s} = T_{\rm a} \quad \text{on} \quad z = 0 \quad \text{for} \quad r > R \quad \text{and} \quad \text{on} \quad z = -h^{\rm s}. \tag{8}$$

Assuming that transport of vapour in the atmosphere is quasi-steady and is solely by diffusion, the concentration of vapour, denoted by $c = c(r, z, t)$, satisfies Laplace's equation $\nabla^2 c = 0$.[19] At the free surface of the droplet we assume that the atmosphere is saturated with vapour and hence

$$c = c_{\rm sat}(T) \quad \text{on} \quad z = h \quad \text{for} \quad r < R, \tag{9}$$

where the saturation value of the concentration $c_{\rm sat} = c_{\rm sat}(T)$ is an increasing function of temperature, approximated quartically in $T_{\rm a} - T$ by

$$c_{\rm sat}(T) = \sum_{i=0}^{4} \alpha_i (T_{\rm a} - T)^i, \tag{10}$$

where the coefficients α_i for $i = 0, \ldots, 4$ were chosen to fit values calculated from the data for the specific volume of water vapour given by Raznjevic[20], leading to $\alpha_0 = 1.93 \times 10^{-2}$, $\alpha_1 = 1.11 \times 10^{-3}$, $\alpha_2 = 2.77 \times 10^{-5}$, $\alpha_3 = 3.80 \times 10^{-7}$ and $\alpha_4 = 2.66 \times 10^{-9}$ in units of kg m^{-3} K^{-i}. Figure 7 shows the quartic approximation (10) together with the corresponding linear and quadratic approximations and the values calculated from the data of Raznjevic[20]. In particular, Figure 7 reveals that while a linear approximation is sufficient for situations with a relatively small evaporative cooling of a few degrees K, such as those considered by David et al.[13] and Dunn et al.[14,15], the quartic approximation (10) is necessary for situations with a larger evaporative cooling of up to 20 K, such as those considered in the present work. On the dry part of the substrate there is no mass flux,

$$\frac{\partial c}{\partial z} = 0 \quad \text{on} \quad z = 0 \quad \text{for} \quad r > R, \tag{11}$$

and, since the chamber is much larger than the droplets used in the experiments, far from the droplet the concentration of vapour approaches its far-field value of zero,

$$c \to 0 \quad \text{as} \quad (r^2 + z^2)^{1/2} \to \infty. \tag{12}$$

Once c is known the local evaporative mass flux from the droplet is given by

$$J = -D\nabla c \cdot \mathbf{n} \quad \text{on} \quad z = h \quad \text{for} \quad r < R, \tag{13}$$

where D is the coefficient of diffusion of vapour in the atmosphere. As discussed in Section I and expressed in equation (2), a standard result from the theory of gases is that D is inversely proportional to pressure, and hence we write

$$D = \frac{D_{\rm ref} p_{\rm ref}}{p_{\rm a}}, \tag{14}$$

where $D_{\rm ref}$ denotes the appropriate reference value of D at the reference pressure $p_{\rm ref} = 1$ atm. Note that the diffusion coefficient is the only parameter in the model that depends on either the nature of the ambient gas or its pressure $p_{\rm a}$.

In the special case $c_{\rm sat} \equiv c_{\rm sat}(T_{\rm a})$, corresponding to setting $\alpha_i = 0$ for $i = 1, \ldots, 4$ in equation (10), the saturation concentration is constant and we recover the basic model in which the problem for the concentration of vapour in the atmosphere is decoupled from the problem for the temperature of the droplet and the substrate. Based on a numerical solution obtained using a finite element method Hu and Larson[7] approximated the evaporation rate in the basic model as

$$-\frac{{\rm d}V}{{\rm d}t} = \frac{\pi R D c_{\rm sat}(T_{\rm a})}{\rho}(0.27\theta^2 + 1.30). \tag{15}$$

This approximation is consistent with the exact analytical results

$$-\frac{{\rm d}V}{{\rm d}t} = \frac{4RDc_{\rm sat}(T_{\rm a})}{\rho} \quad \text{when} \quad \theta = 0 \tag{16}$$

and

$$-\frac{{\rm d}V}{{\rm d}t} = \frac{2\pi RDc_{\rm sat}(T_{\rm a})}{\rho} \quad \text{when} \quad \theta = \frac{\pi}{2} \tag{17}$$

for the basic model, and provides a useful check on the accuracy of the numerical procedure in this case.

In general, the problem for the vapour concentration c is coupled to the problem for the temperatures T and $T^{\rm s}$ and has to be solved numerically. This was done using the

MATLAB-based finite element package COMSOL Multiphysics (formerly FEMLAB), using a semi-circular domain whose radius was chosen to be 320 times the radius of the droplet and mesh points that were much more densely populated near the contact line. Comparison with equation (17) in the special case $c_{\mathrm{sat}} \equiv c_{\mathrm{sat}}(T_{\mathrm{a}})$ suggests that this procedure entails at most a 1% numerical error. At each time step the system of equations described above was solved to obtain $\mathrm{d}V/\mathrm{d}t$. Euler's forward method was then used to estimate V, and hence θ and h, and hence the geometry at the next time step.

IV. EXPERIMENTAL RESULTS AND COMPARISON WITH MODEL

As the typical experimentally measured evolutions in time of the volume and the base radius of a droplet shown in Figure 4 illustrate, typically the evaporation process can be divided into two stages. In the first stage, the droplet is pinned and so the base radius is constant while the volume decreases very nearly linearly in time and hence the evaporation rate is very close to being constant in time. In the second stage, the droplet depins and so both the base radius and the volume decrease until complete evaporation. Henceforth we will restrict our attention to the first stage, i.e. to the situation in which the droplet is pinned and the evaporation rate is very close to being constant in time, and hence it is sufficient to use the average evaporation rate, which both the basic model and experimental studies, such as that by Birdi et al.[12], indicate is proportional to the perimeter of the base of the droplet.

Figure 8 shows the effect of reducing the atmospheric pressure on the experimentally measured evaporation rate of droplets of water on an aluminium substrate in an atmosphere of nitrogen. The evaporation rate increases from around 3 nl s^{-1} at atmospheric pressure to more than 40 nl s^{-1} at the lowest pressure investigated (around 40 mbar). On a logarithmic scale the experimental data can be reasonably approximated by a straight line, leading to a simple numerical fit in the form $-\mathrm{d}V/\mathrm{d}t = \alpha p_{\mathrm{a}}^{\beta}$, where α and $\beta \simeq -0.941$ are fitting parameters, which is also shown in Figure 8. The inset in Figure 8 shows the same results plotted on a linear (rather than a logarithmic) scale. The corresponding approximations for evaporation into the other two ambient gases studied (not shown for brevity) yield $\beta \simeq -0.867$ for helium and $\beta \simeq -0.873$ for carbon dioxide, confirming that the evaporation rate and hence the diffusion coefficient are indeed approximately inversely proportional to

Ambient Gas	He	N_2	CO_2
Diffusion Coefficient (m^2 s^{-1})	6.61×10^{-5}	2.15×10^{-5}	1.23×10^{-5}

TABLE III: The fitted reference values of the diffusion coefficients of water vapour into the ambient gases used in the experiments, $D_{\rm ref}$, at pressure 1 atm and temperature 295 K.

pressure, as assumed in the mathematical model.

In what follows we compare the experimental results with the corresponding theoretical predictions of the mathematical model described in Section III.

Figure 9 shows the effect of reducing the atmospheric pressure on the experimentally measured evaporation rate of droplets of water on an aluminium substrate in atmospheres of helium, nitrogen and carbon dioxide. In particular, Figure 9 illustrates that for a given substrate (in this case aluminium, but the same trend occurs for the other substrates studied) ambient gases with higher diffusion coefficients showed higher evaporation rates. Figure 9 also shows (as dashed lines) the theoretical predictions of the mathematical model using the parameter values given in Section III and reveals that, while the predictions of the model are qualitatively correct, they tend to over-predict the evaporation rate somewhat, and so in order to improve the quantitative predictions of the model a simple fitting of the value of the diffusion coefficient was performed. Specifically, for each of the ambient gases studied the value of the diffusion coefficient at the reference pressure (i.e. $D_{\rm ref}$ in equation (14)) was fitted by comparing the experimental results for evaporation on an aluminium substrate with the corresponding theoretical predictions. Figure 9 also shows (as solid lines) the fitted theoretical predictions of the mathematical model and demonstrates that by tuning the value of a single parameter for each ambient gas we were able to obtain good agreement between theory and experiment across the entire range of atmospheric pressures studied. The fitted reference values of the diffusion coefficients of the ambient gases used in the experiments are given in Table III, and vary by at most 20% from the values given in Table II, i.e. comparable with the uncertainty in the theoretical values.

Thus far we have restricted our discussion to the case of a substrate that is a good thermal conductor, namely aluminium. The present investigation also included other substrates with a wide range of thermal conductivities, and so Figures 10 – 12 show both the experimental results and the corresponding theoretical predictions of the mathematical model for all four substrates studied for atmospheres of helium, nitrogen and carbon dioxide, respectively.

Figures 10 – 12 contain many of the main results of the present work and show some very clear trends. In particular, they show that for all the combinations of ambient gases and substrates studied, reducing the atmospheric pressure increases the evaporation rate. Furthermore, droplets on substrates with higher thermal conductivities evaporate more quickly than those on substrates with lower thermal conductivities, although the differences are less marked for ambient gases with smaller diffusion coefficients (e.g. the differences for helium shown in Figure 10 are more significant than those for carbon dioxide shown in Figure 12). Figures 10 – 12 also show that the theoretical predictions of the mathematical model using the values of the diffusion coefficients fitted for an aluminium substrate are in reasonable agreement with the experimental results for the other three substrates studied. (Obviously we could obtain even better agreement if we fitted the values of the diffusion coefficients separately for each substrate, but since the value of the diffusion coefficient should be independent of the nature of the substrate we chose not to do this.) Inspection of Figures 10 – 12 reveals that the agreement between theory and experiment is poorest for the substrate with the lowest thermal conductivity (namely PTFE), and the deviation is more pronounced for ambient gases with larger diffusion coefficients and at lower atmospheric pressures. Figures 10 – 12 also show that the corresponding predictions of the basic model, which are independent of the thermal properties of the droplet and the substrate, consistently over-predict the evaporation rate.

As we have seen, Figures 10 – 12 show that as the atmospheric pressure is reduced both the differences between the evaporation rates from droplets on different substrates and the differences between theory and experiment become more pronounced. Experimental measurements of the bulk temperature within the droplets help us to understand the intimate link between temperature and evaporation. Figure 13 shows the experimentally measured evaporative cooling, ΔT, defined to be the difference between the atmospheric temperature and the bulk temperature, plotted as a function of the atmospheric pressure for the most and least thermally conducting substrates (namely aluminium and PTFE) in an atmosphere of helium. In particular, Figure 13 shows that, as expected, the evaporative cooling is more pronounced on the substrate with the lowest thermal conductivity (namely PTFE) and less pronounced on the substrate with the highest thermal conductivity (namely aluminium). Figure 13 also shows that for both substrates the evaporative cooling increases substantially as the atmospheric pressure is reduced. Indeed, very large evaporative cooling of the order

of 20 K was observed at the lowest values of pressure investigated (around 40 mbar). A comparison between the experimental results shown in Figure 13 and the corresponding theoretical predictions of the mathematical model will be presented in Section V.

V. DISCUSSION

As described earlier, when a liquid droplet is deposited on a substrate in an unsaturated atmosphere it will spontaneously evaporate. In many situations, including those investigated in the present work, the rate-limiting step for evaporation is the diffusive relaxation of the locally saturated vapour at the free surface of the droplet to its far-field value and so, as we have seen, the coefficient of diffusion of vapour in the atmosphere plays a key role. As we have described theoretically and demonstrated from the experimental results in Section IV, the diffusion coefficients are inversely proportional to the atmospheric pressure and depend on the nature of the ambient gas, and the fitted values of the diffusion coefficient at atmospheric pressure differ by up to only 20% from the experimental ones. Since the diffusion coefficient D plays such a key role, the experimentally measured evaporation rates for droplets in atmospheres of *all* three ambient gases on *all* four substrates are plotted as functions of D in Figure 14. Figure 14 also includes the corresponding theoretical predictions of the mathematical model and of the basic model. This novel presentation of all of our results in a single plot reveals some important trends. In particular, it reveals that for each substrate the evaporation rate is an increasing function of D. The experimental results and the predictions of the mathematical model (which, as we have seen, incorporates the effects of evaporative cooling via the temperature dependence of the saturation value of the concentration) show that droplets on substrates with higher thermal conductivities evaporate more quickly than those on substrates with lower thermal conductivities. Figure 14 shows that theory and experiment are in good agreement at lower values of D, but the mathematical model systematically over-predicts the experimental results at larger values of D. The prediction of the basic model (which, as we have seen, decouples the concentration of vapour in the atmosphere from the temperature of the droplet and hence does not account for the effect of the thermal properties of the substrate on the evaporation rate) is simply linear in D in accord with equations (15) – (17) and significantly over-predicts the evaporation rate.

In addition to evaporation rates, the mathematical model can also predict temperature

within the droplet, and a comparison of these predictions with experimental measurements is a good test of the validity of the model. Figure 15 shows a comparison between the experimental measurements and the corresponding theoretical predictions of the evaporative cooling, ΔT, as a function of the atmospheric pressure for droplets on aluminium and PTFE substrates evaporating in an atmosphere of helium. For this purpose the theoretical value of the bulk temperature was defined to be

$$\frac{1}{h_{\mathrm{m}}(0)} \int_0^{h_{\mathrm{m}}(0)} T(0, z, 0)\, \mathrm{d}z, \tag{18}$$

where h_{m} is again the maximum height of the droplet. Considering the approximations made in deriving the mathematical model, the fact that it captures the qualitative trend and order of magnitude of the experimental results is rather encouraging. One obvious uncertainty in the comparison shown in Figure 15 is the exact location at which the temperature is measured in the experiments (see, for example, the measurements of temperatures at different locations within an evaporating droplet reported by David et al.[13]), and how this relates to the average value of the temperature calculated theoretically according to (18). Both of these aspects could be improved in future studies.

As Figures 10 – 13 show, the agreement between theory and experiment is poorest for substrates with the lowest thermal conductivities, and the deviation is more pronounced for ambient gases with larger diffusion coefficients and at lower atmospheric pressures, i.e. situations with the largest evaporation rates and strongest evaporative cooling.

Perhaps the most likely cause of the poorer agreement in situations with larger evaporation rates is the presence of thermocapillary-driven (Marangoni) flow within the droplet. Thermocapillary-driven flows within evaporating droplets have recently been studied by several authors, including Hu and Larson[21], Ristenpart et al.[22] and Xu and Luo[23]. However, the excellent agreement between their theory and experiments conducted at atmospheric pressure led Dunn et al.[14,15] to suggest that thermocapillary effects were probably not significant in these experiments, a conclusion subsequently confirmed by the results of the numerical computations undertaken by Girard et al.[24]. However, stronger evaporation will tend to enhance the thermocapillary effect, making it a potential cause of the poorer agreement.

Another possible cause of the poorer agreement between theory and experiment in situations with stronger evaporation could be that the evaporative cooling may not be entirely compensated by the heat conduction through the substrate as assumed in the mathematical

model, leading to non-equilibrium effects at the free surface of the droplet (as discussed by, for example, Sultan et al.[25]).

VI. CONCLUSIONS

An experimental and theoretical study into the effect of the atmosphere on the evaporation of pinned sessile droplets of water has been described. The experimental work investigated the evaporation rates of sessile droplets in atmospheres of three different ambient gases at reduced pressure using four different substrates with a wide range of thermal conductivities. Reducing the atmospheric pressure increases the diffusion coefficient of water vapour in the atmosphere and hence increases the evaporation rate. Changing the ambient gas also alters the diffusion coefficient and hence also affects the evaporation rate. A mathematical model that takes into account the effect of the atmospheric pressure and the nature of the ambient gas on the diffusion of water vapour in the atmosphere was developed, and its predictions were found to be in encouraging agreement with the experimental results. A more refined mathematical model incorporating thermocapillary and non-equilibrium effects would probably yield significantly improved theoretical predictions for the evaporation rate and the evaporative cooling of rapidly evaporating droplets.

Acknowledgments

The present work was supported by the United Kingdom Engineering and Physical Sciences Research Council (EPSRC) via joint research grants GR/S59444 (Edinburgh) and GR/S59451 (Strathclyde). The first author (KS) gratefully acknowledges valuable discussions with Prof. L. Tadrist (Laboratoire IUSTI, Marseille, France).

---

[1] J. C. Maxwell, "Diffusion" in *The Scientific Papers of James Clerk Maxwell, Vol. 2*, ed. W. D. Niven (Cambridge University Press, 1890, reprinted Dover, New York, 1952). pp. 625–646.

[2] I. Langmuir, "Evaporation of small spheres", Phys. Rev. **12**, 368 (1918).

[3] R. G. Picknett and R. Bexon, "The evaporation of sessile or pendant drops in still air," J. Coll. Int. Sci. **61**, 336 (1977).

[4] C. Bourgès-Monnier and M. E. R. Shanahan, "Influence of evaporation on contact angle," Langmuir **11**, 2820 (1995).

[5] C. Poulard, O. Bénichou, and A. M. Cazabat, "Freely receding evaporating droplets," Langmuir **19**, 8828 (2003).

[6] R. Deegan, "Pattern formation in drying drops," Phys. Rev. E **61**, 475 (1998).

[7] H. Hu and R. G. Larson, "Evaporation of a sessile droplet on a substrate," J. Phys. Chem. B **106**, 1334 (2002).

[8] Y. O. Popov, "Evaporative deposition patterns: spatial dimensions of the deposit," Phys. Rev. E **71**, 036313 (2005).

[9] C. Poulard, G. Guéna, and A. M. Cazabat, "Diffusion-driven evaporation of sessile drops," J. Phys.: Condens. Matter **17**, S4213 (2005).

[10] N. Shahidzadeh-Bonn, S. Rafaï, S., A. Azouni, and D. Bonn, "Evaporating droplets," J. Fluid Mech. **549**, 307 (2006).

[11] G. Guéna, C. Poulard, and A. M. Cazabat, "The leading edge of evaporating droplets," J. Coll. Int. Sci. **312**, 164 (2007).

[12] K. S. Birdi, D. T. Vu, and A. Winter, "A study of the evaporation rates of small water drops placed on a solid surface," J. Phys. Chem. **93**, 3702 (1989).

[13] S. David, K. Sefiane, and L. Tadrist, "Experimental investigation of the effect of thermal properties of the substrate in the wetting and evaporation of sessile drops," Colloids and Surfaces A: Physiochem. Eng. Aspects **298**, 108 (2007).

[14] G. J. Dunn, S. K. Wilson, B. R. Duffy, S. David, and K. Sefiane, "A mathematical model for the evaporation of a thin sessile liquid droplet: comparison between experiment and theory," Colloids and Surfaces A: Physiochem. Eng. Aspects **323**, 50 (2008).

[15] G. J. Dunn, S. K. Wilson, B. R. Duffy, S. David, and K. Sefiane, "The strong influence of substrate conductivity on droplet evaporation," J. Fluid Mech. **623**, 329 (2009).

[16] R. C. Reid, J. M. Prausnitz, and B. E. Poling, *The Properties of Gases and Liquids*, 4th edn. (McGraw-Hill, New York, 1987).

[17] C. A. Ward and F. Duan, "Turbulent transition of thermocapillary flow induced by water evaporation," Phys. Rev. E **69**, 056308 (2004).

[18] The assumption that the droplet shape can be approximated by a spherical cap is appropriate when the base radius of the droplet is less than the capillary length, $\ell = (\gamma/\rho g)^{1/2} \simeq 3$ mm,

which holds for the droplets considered in the present work.

[19] The assumption that the transport of vapour in the atmosphere is quasi-steady is appropriate when the characteristic timescale for diffusion, R^2/D, where D is the coefficient of diffusion of vapour in the atmosphere, is much less than the lifetime of the droplet, a condition that is amply satisfied even at the lowest pressures (and hence highest evaporation rates) considered in the present work.

[20] K. Raznjevic, *Handbook of Thermodynamic Tables*, 2nd ed. (Begell House, New York, 1995). Table 3-1, p. 85.

[21] H. Hu and R. G. Larson, "Marangoni effect reverses coffee-ring depositions," J. Phys. Chem. B **110**, 7090 (2006).

[22] W. D. Ristenpart, P. G. Kim, C. Domingues, J. Wan, and H. A. Stone, "Influence of substrate conductivity on circulation reversal in evaporating drops," Phys. Rev. Lett. **99**, 234504 (2007).

[23] X. Xu and J. Luo, "Marangoni flow in an evaporating water droplet," Appl. Phys. Lett. **91**, 124102 (2007).

[24] F. Girard, M. Antoni, and K. Sefiane, "On the effect of Marangoni flow on evaporation rates of heated water drops," Langmuir **24**, 9207 (2008).

[25] E. Sultan, A. Boudaoud, and M. Ben Amar, "Evaporation of a thin film: diffusion of the vapour and Marangoni instabilities," J. Fluid Mech. **543**, 183 (2005).

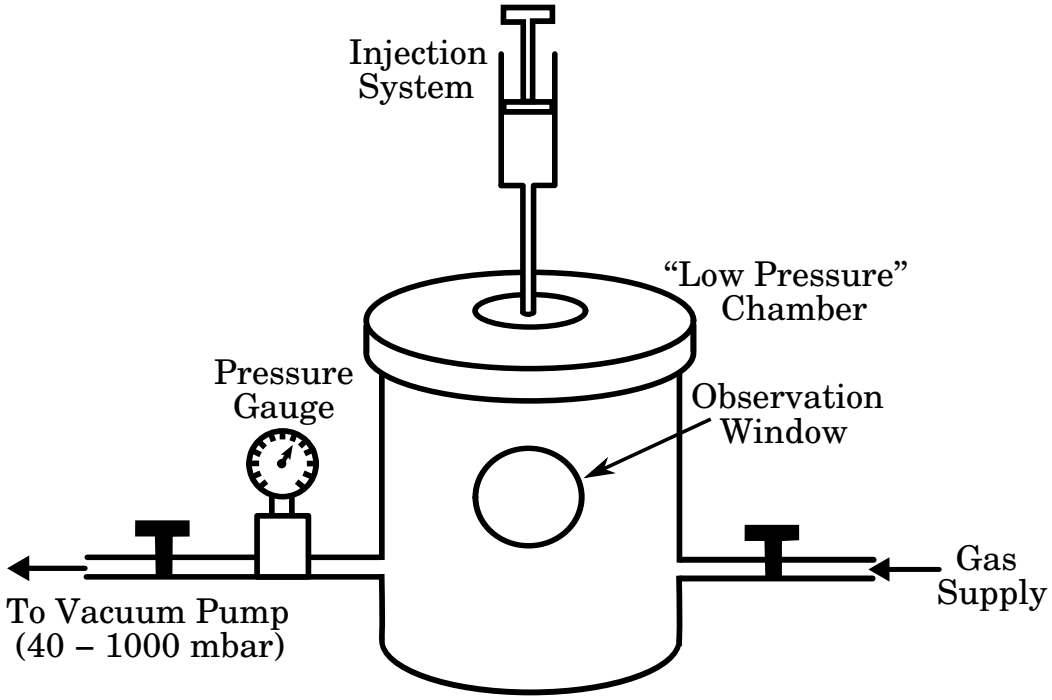

FIG. 1: `lowpressurechamber.eps` The "low pressure" chamber connected to a gas supply and a vacuum pump.

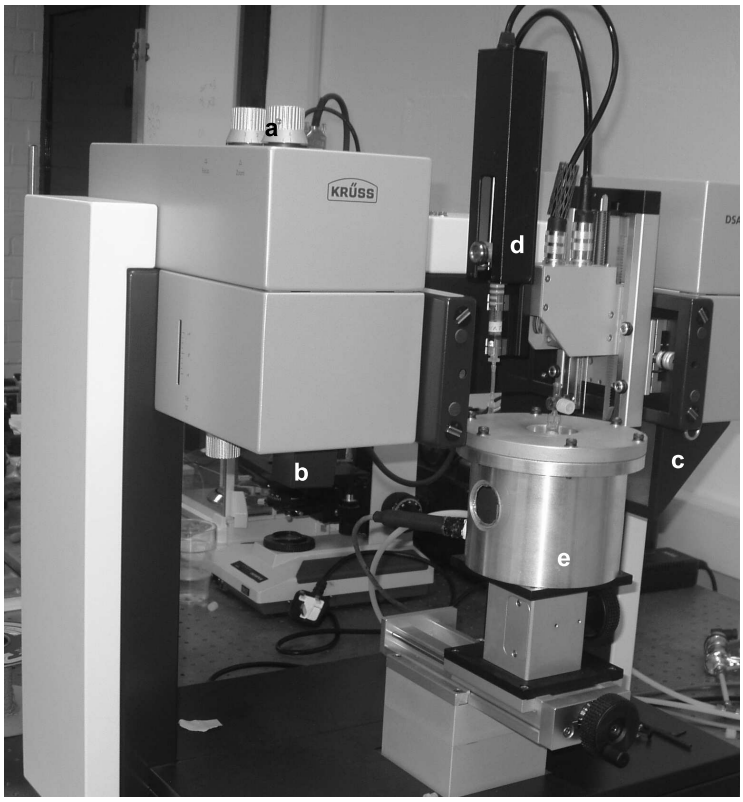

FIG. 2: apparatus.eps The DSA100^{TM} Droplet Shape Analysis (DSA) system with the "low pressure" chamber: (a) focus and magnification adjustment knobs, (b) charge-coupled device (CCD) camera, (c) light source, (d) injection system, and (e) low pressure chamber on the three-axis stage.

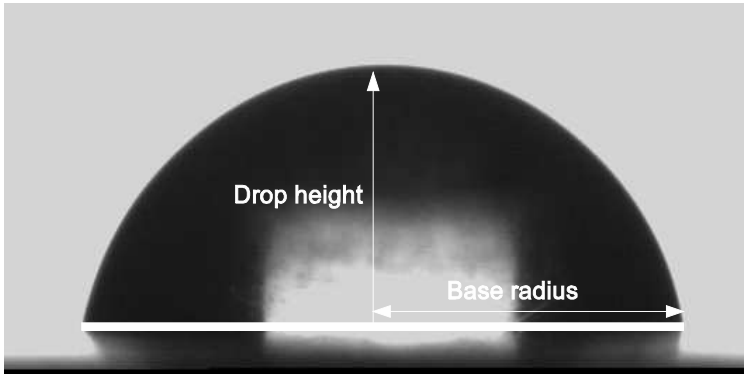

FIG. 3: `droplet.eps` An example of a droplet of water on an aluminium substrate.

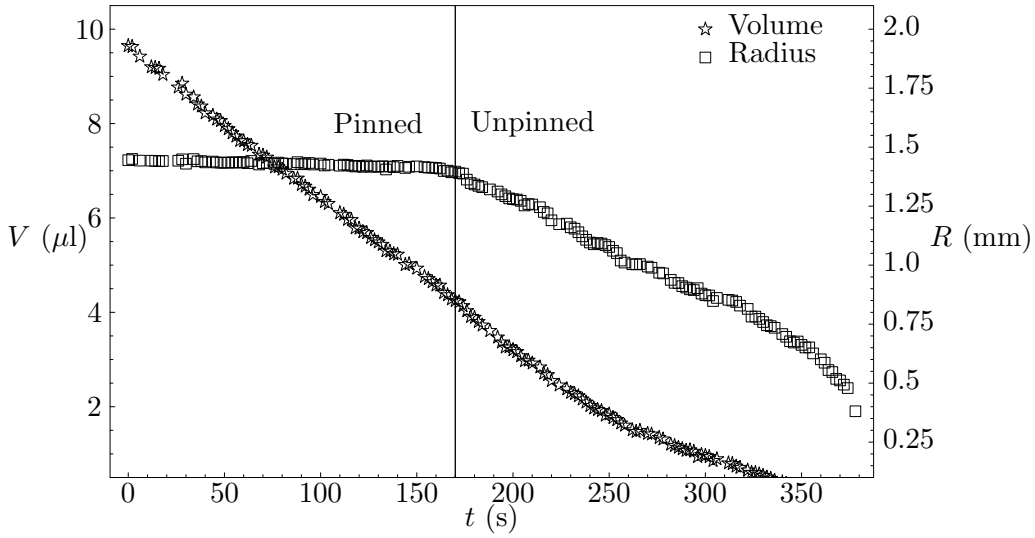

FIG. 4: VolRadEvo.eps Typical examples of the experimentally measured evolutions in time of the volume (left hand axis) and the base radius (right hand axis) of a droplet of water on an aluminium substrate evaporating into an atmosphere of nitrogen at low pressure.

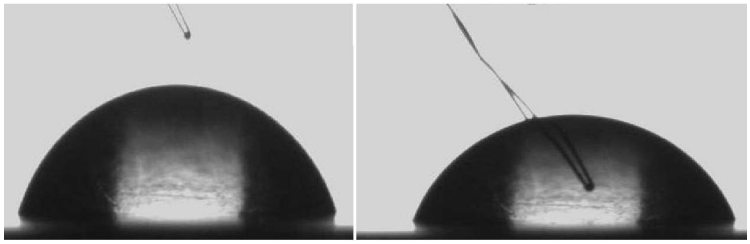

FIG. 5: thermocouple.eps Example of the insertion of a miniature thermocouple into a droplet in order to measure the bulk temperature.

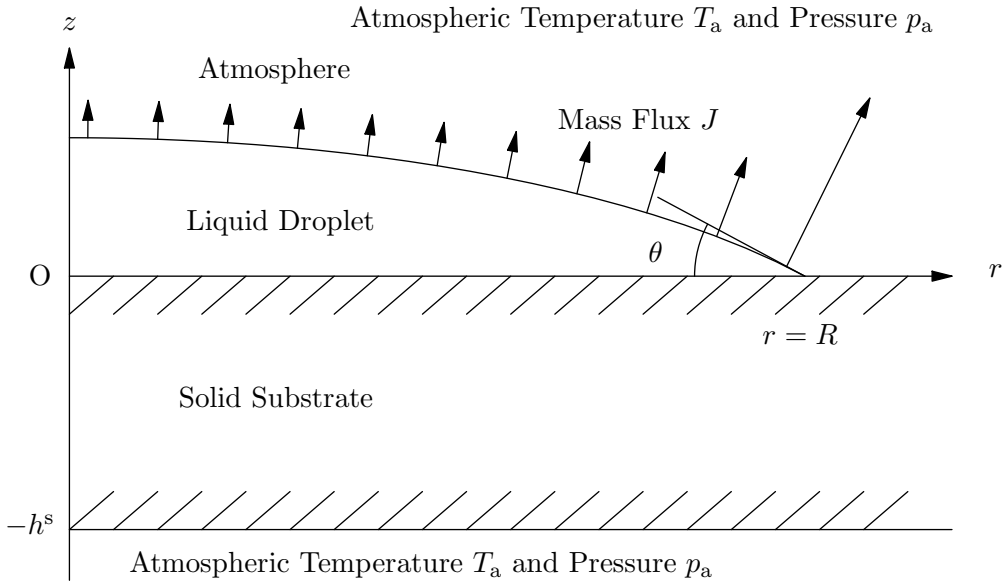

FIG. 6: geom.eps Geometry of the mathematical model.

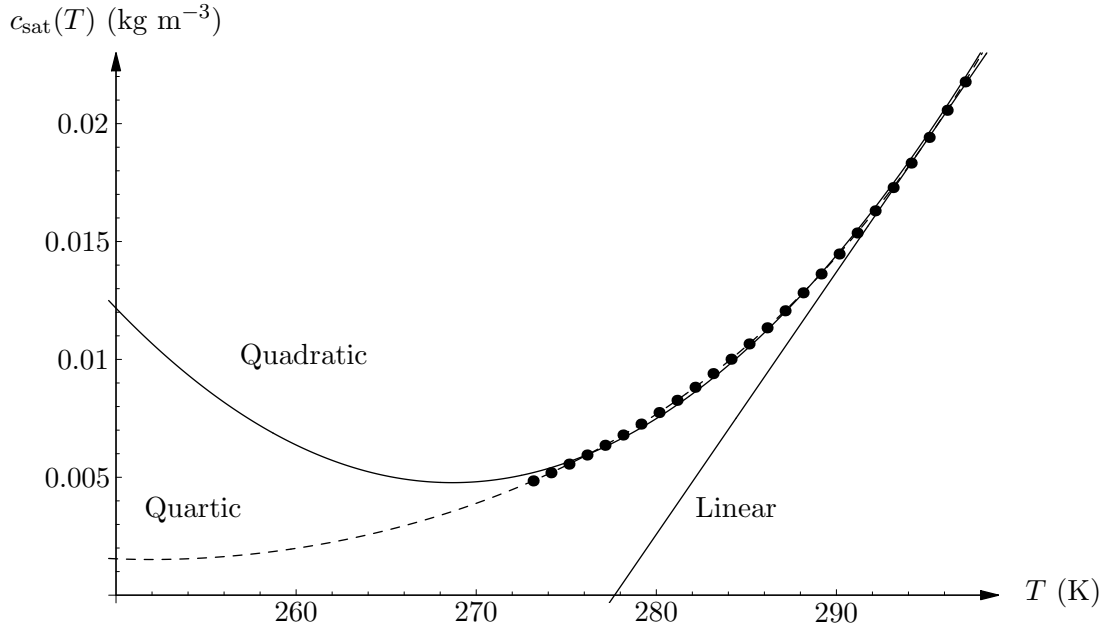

FIG. 7: cvTv2.eps Variation of the saturation concentration of vapour $c_{\mathrm{sat}}(T)$ with temperature T showing the quartic approximation (10) (marked with the dashed line) together with the corresponding linear and quadratic approximations (marked with solid lines) and the values calculated from the data given by Raznjevic[20] (marked with dots).

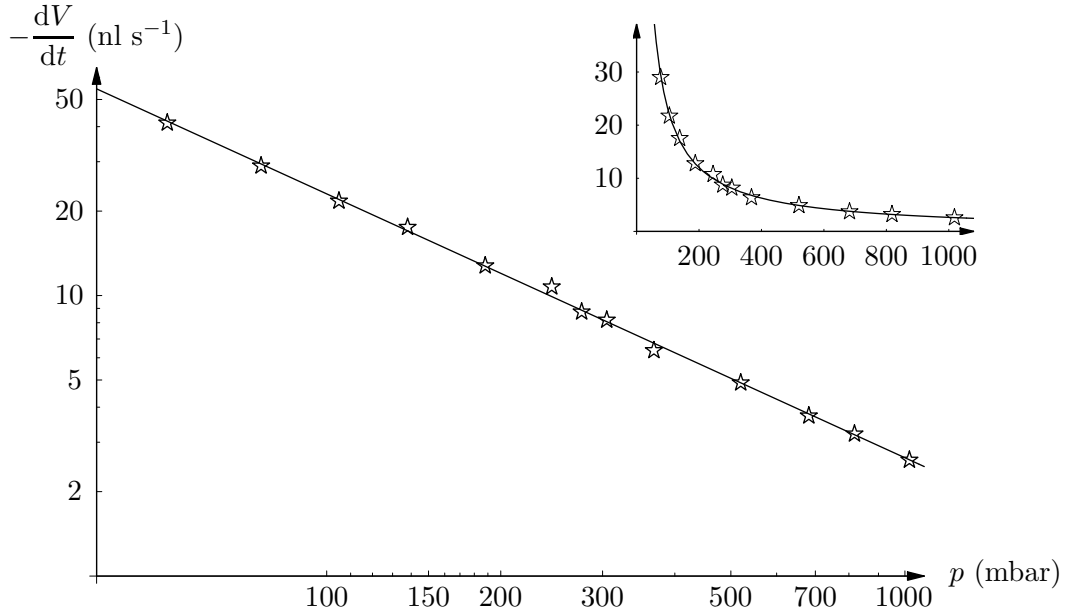

FIG. 8: LFitLogLogNitAlEvpLINS.eps Experimentally measured evaporation rates of droplets of water on an aluminium substrate in an atmosphere of nitrogen for different atmospheric pressures. The inset shows the same data on a linear (rather than a logarithmic) scale. In both plots the line is a simple numerical fit to the experimental data.

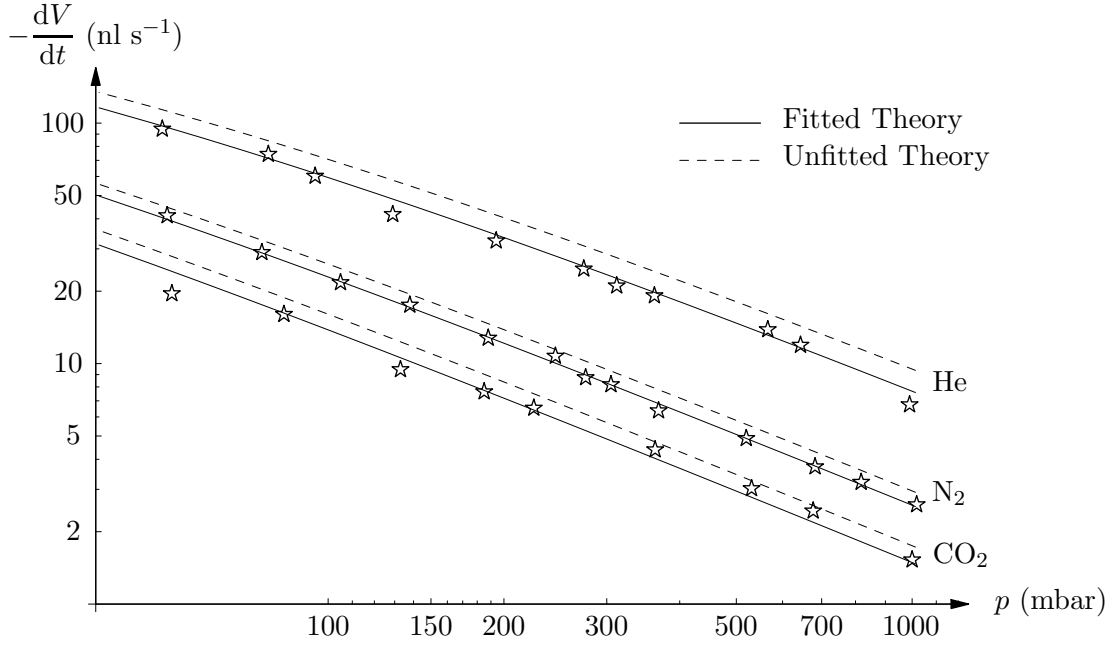

FIG. 9: CombLogLogAlEvp.eps Experimentally measured evaporation rates of droplets of water on an aluminium substrate in atmospheres of helium, nitrogen and carbon dioxide for different atmospheric pressures, together with the corresponding theoretical predictions of the mathematical model using the parameter values given in Section III ("Unfitted Theory", marked with a dashed line) and using the fitted reference values of the diffusion coefficients given in Table III ("Fitted Theory", marked with a solid line).

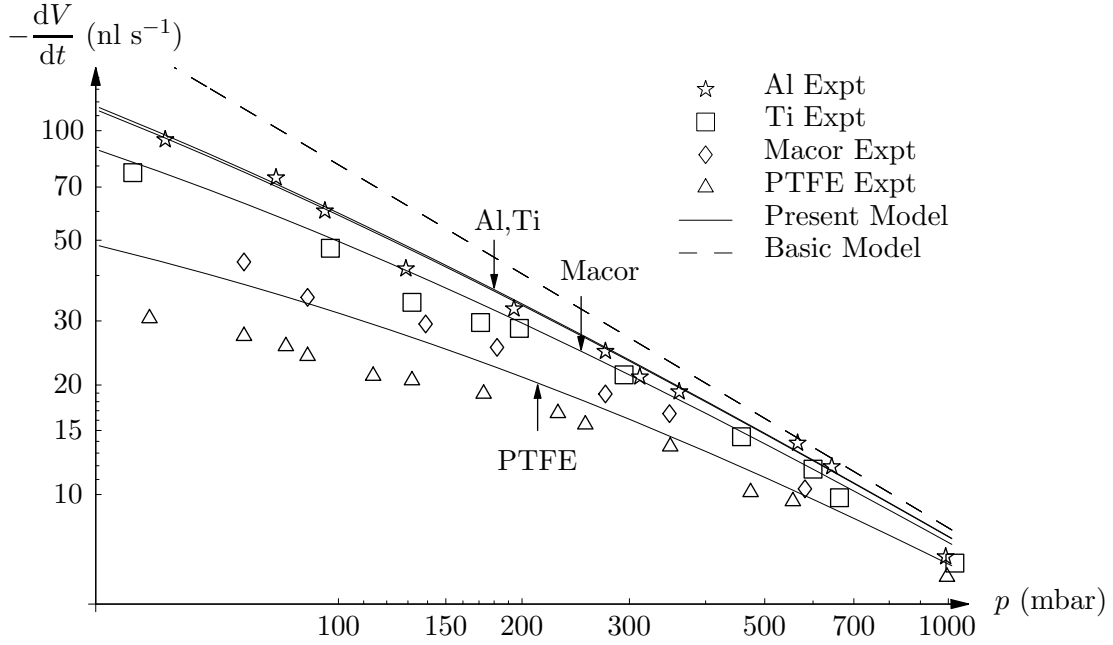

FIG. 10: DFitLogLogHelEvpv2.eps Experimentally measured evaporation rates of droplets of water in an atmosphere of helium on various substrates for different atmospheric pressures, together with the corresponding theoretical predictions of the mathematical model and the basic model.

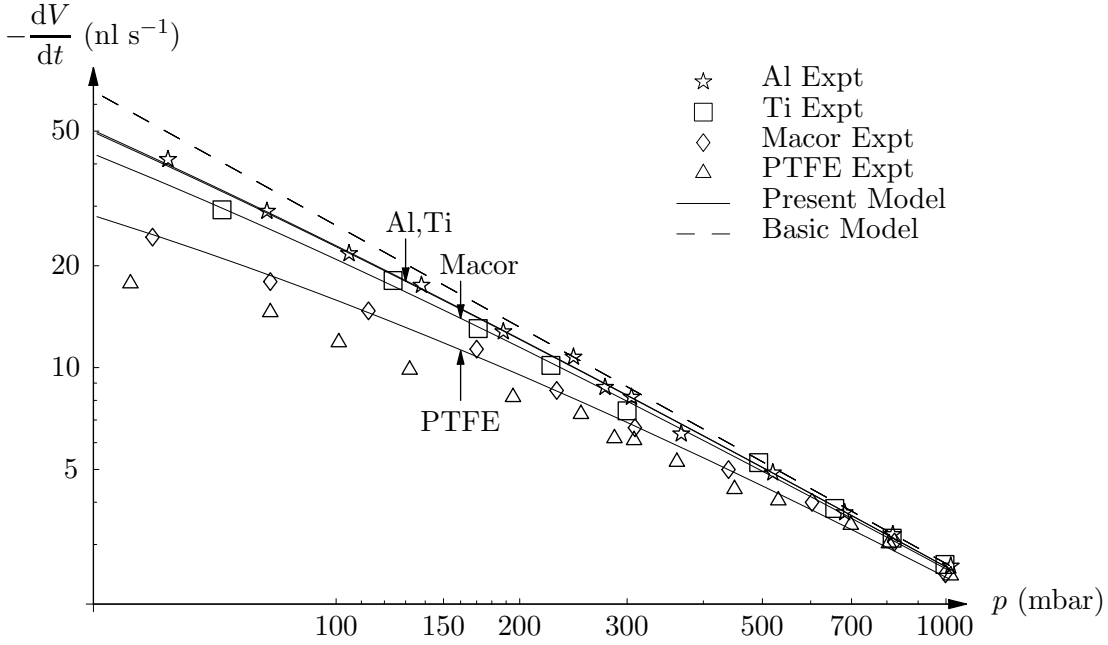

FIG. 11: DFitLogLogNitEvpv2.eps As Figure 10, except in an atmosphere of nitrogen.

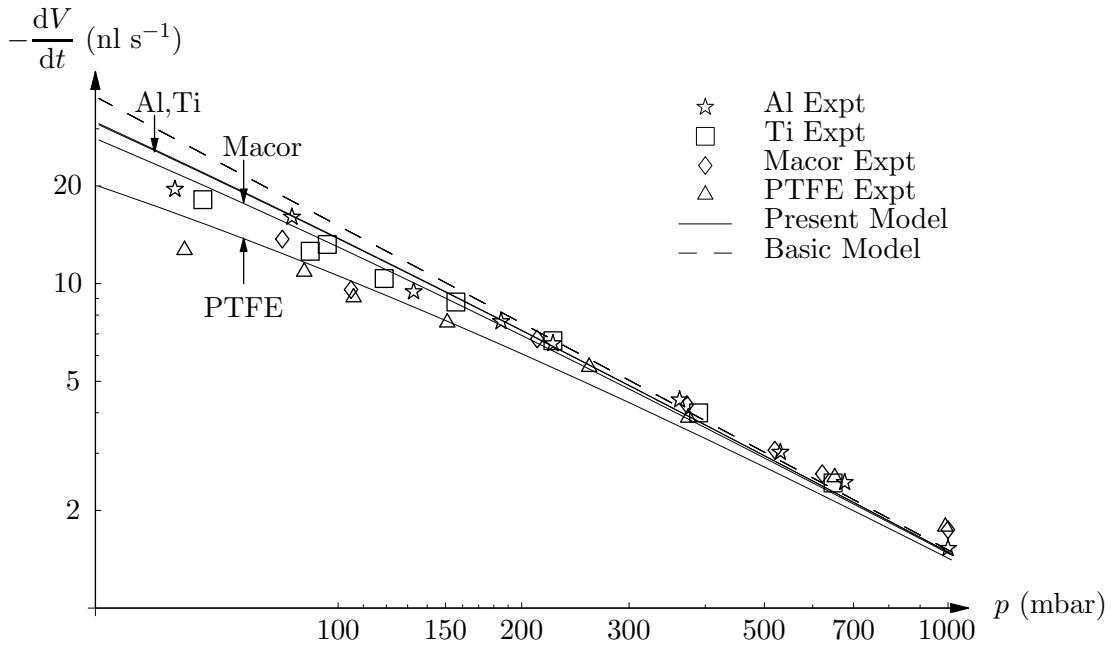

FIG. 12: `DFitLogLogCO2Evpv2.eps` As Figure 10, except in an atmosphere of carbon dioxide.

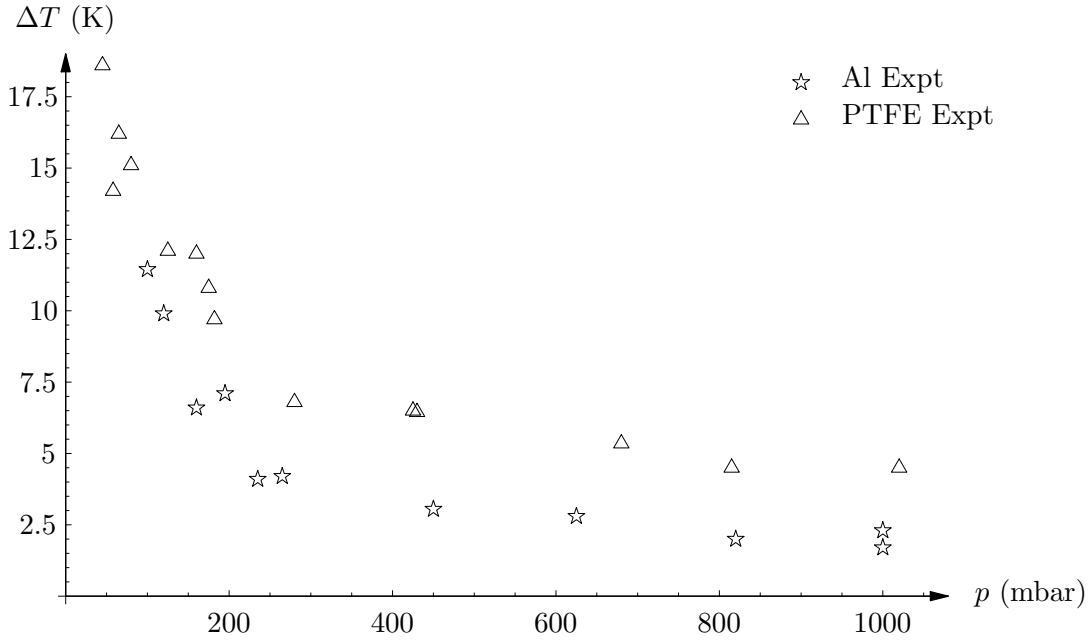

FIG. 13: `ExpHelTvp.eps.eps` Experimentally measured evaporative cooling of droplets of water in an atmosphere of helium on aluminium and PTFE substrates for different atmospheric pressures.

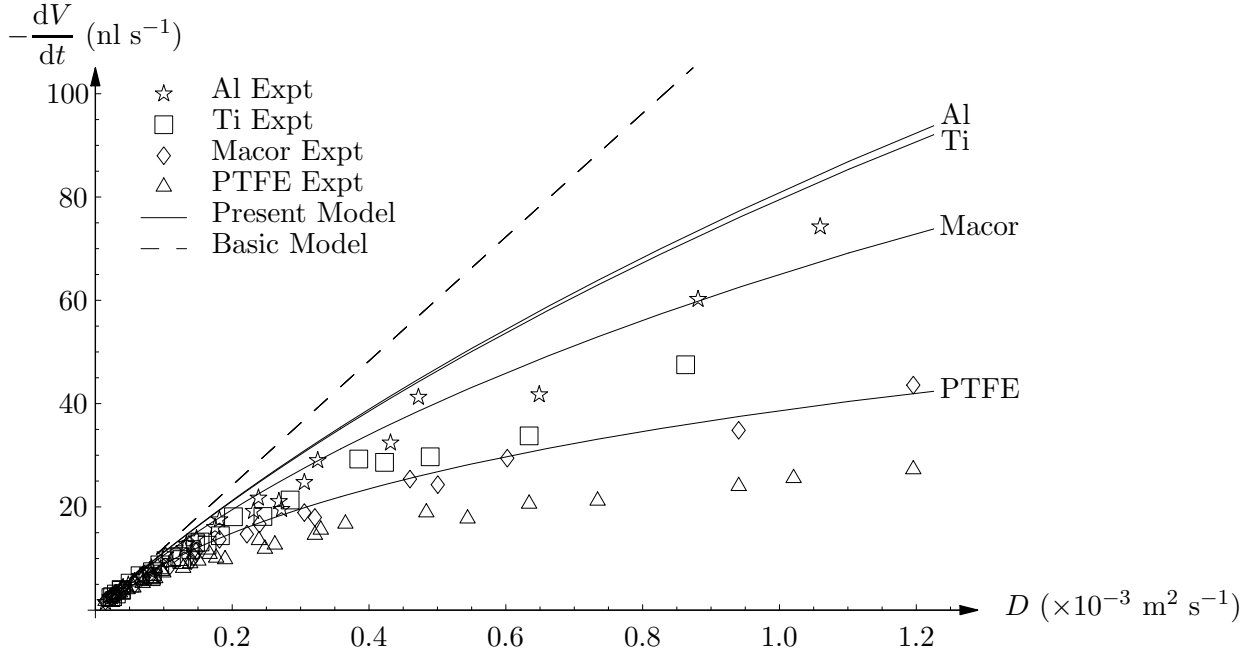

FIG. 14: DFitEvD.eps Experimentally measured evaporation rates of droplets of water in atmospheres of all three ambient gases on all four substrates plotted as functions of the diffusion coefficient D together with the corresponding theoretical predictions of the mathematical model and the basic model.

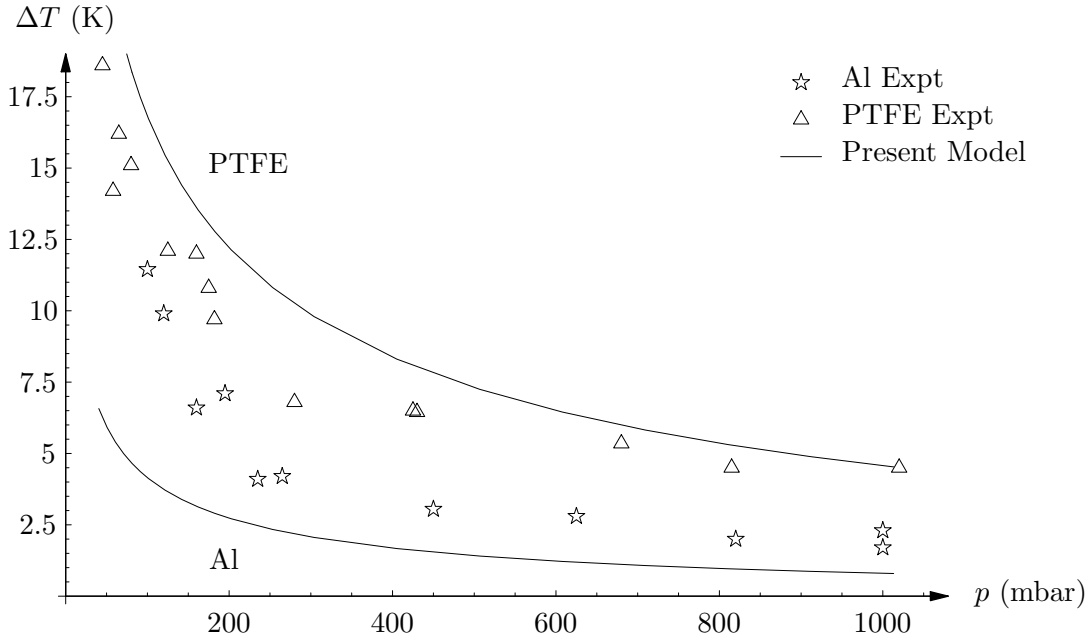

FIG. 15: DFitHelTvp.eps Comparison between the experimentally measured evaporative cooling of droplets of water in an atmosphere of helium on aluminium and PTFE substrates for different atmospheric pressures shown in Fig. 13 and the corresponding theoretical predictions of the mathematical model.